XIX IMEKO World Congress
Fundamental and Applied Metrology
September 6–11, 2009, Lisbon, Portugal

EXPERIMENTAL EVALUATION OF THE CLAMPING PRESSURE DISTRIBUTION IN A PEM FUEL CELL USING MATRIX-BASED PIEZORESISTIVE THIN-FILM SENSORS

R. Montanini [1], *G. Squadrito* [2], *G. Giacoppo* [2]

[1] Faculty of Engineering, University of Messina, Messina, Italy, rmontanini@ingegneria.unime.it
[2] CNR Institute for Transformation and Storage of Energy, Messina, Italy, gaetano.squadrito@itae.cnr.it
giosue.giacoppo@itae.cnr.it

Abstract – The achievement of a proper and uniform pressure distribution between the membrane electrode assembly (MEA) and the bipolar plates of a proton exchange membrane fuel cell (PEMFC) is a key factor of stack design and assembly. Contact pressure levels are usually controlled by selecting an appropriate external clamping pressure on the endplates. Very few studies have been focused on the measurement of the contact pressure distribution within the fuel cell and its correlation with the applied external clamping torque. This study explores the possibility of using matrix-based piezoresistive thin-film sensors, to be placed between the MEA and the monopolar plate of a PEMFC, to investigate this correlation. Before embedding the sensor array into the fuel cell, it was validated for accuracy and repeatability by designing a pneumatic calibration device which allows to apply uniform static pressure levels over the whole sensor area. Preliminary results reported in this study showed that, as the clamping torque on the endplates is increased, the average pressure on the MEA remains almost constant but its distribution changes. The core area of the electrode becomes progressively more unloaded while average stresses on the gasket rise up, with significant stress concentration around the edge corners.

Keywords: PEM fuel cells, contact pressure mapping, matrix-based piezoresistive thin-film sensors

1. INTRODUCTION

Proton exchange membrane fuel cell (PEMFC) is an emerging technology that converts the chemical energy stored in hydrogen and oxygen into electricity, with very low pollutants generation. The stacking design and cell assembly parameters significantly affect the electro-chemical performance of PEMFC [1-4], governing the ohmic and mass transport polarizations inside the fuel cell.

One of the most important goals in stack design and assembly is to achieve a proper and uniform pressure distribution between the membrane electrode assembly (MEA) and the bipolar plates. Uneven distribution of the contact pressure will result in hot spots which may have a detrimental effect on PEMFC electro-chemical performance and life. For a given stacking design, contact pressure levels are usually controlled by selecting an appropriate external clamping pressure on the endplates. An insufficient clamping pressure may result in sealing problems, such as fuel leakage, internal crossover and high contact resistance between the gas diffusion layer (GDL) and the bipolar plates. On the other hand, a high clamping pressure may squeeze the relatively thin GDL and change its porosity and permeability, choking the flow of gases and making the migration of water difficult.

Very little scientific research has been focused on the measurement of the contact pressure distribution within the fuel cell and its correlation with the applied clamping torque.

Chang et al. [5] studied the effects of the clamping pressure on the performance of a PEMFC. The electro-physical properties of a carbon paper gas diffusion layer (i.e., porosity, gas permeability, electrical resistance and thickness) were measured using a special designed test rig. Empirical correlations for the gas permeability and the electrical resistance of the GDL were found in terms of the clamping pressure level. Results showed that a low clamping pressure (< 5 bar) results in a high interfacial resistance between the bipolar plate and the gas diffusion layer that reduces the electrochemical performance of the fuel cell. In contrast, a high clamping pressure (> 10 bar) reduces the contact resistance between the graphite plate and the gas diffusion layer, but meanwhile narrows down the diffusion path for mass transfer from gas channels to the catalyst layers. However, the experimental tests were carried out on a test stand simulating the actual behaviour of a PEMFC and no information about the internal contact pressure distribution was provided.

Recently, Wang et al. [6] used pressure sensitive Fuji films (Fuji Photo Co., Ltd, Tokyo, Japan) inserted between the MEA and the diffusion layer of a PEMFC to measure the pressure distribution of both conventional and newly designed hydro-pressurized endplates. It was found that by pressurizing the built-in pocket with hydraulic fluid, the pressure distribution over the fuel cell active area could be improved and fuel cell performance enhanced. The study was focused on the comparison between conventional and newly designed endplates rather than on the actual pressure distribution produced by different clamping pressure levels.

ISBN 978-963-88410-0-1

Lee et al. [7] used finite element analysis (FEA) procedures to simulate the cell stack assembly of a single PEMFC with metallic bipolar plates. The contours of pressure distribution and compliance were obtained for key components such as the MEA and the gas diffusion layer. From these results, the effects of stack design and cell assembly procedures on stack integrity could be evaluated. In order to verify the results of the analysis, experimental tests, using a Fuji pre-scale pressure film inserted between the bipolar plates and the MEA, were conducted to establish the actual pressure distribution at four different clamping pressure levels. The calculated pressure contours were very similar to the experimental measurements, but the percentage error between the measured and simulated pressure values was quite large (10 – 60%). Moreover, the use of pre-scale pressure films, that saturate as the maximum pressure had been reached, did not allow pressure relaxations to be measured as the clamping pressure changed, thus hiding important information.

The goal of this study is to develop a consistent method to measure the contact pressure distribution within a fuel cell and to allow real-time continuous data acquisition as the clamping pressure is varied. The proposed methodology relies on distributed matrix-based piezoresistive thin-film sensors to be interposed between the membrane electrode assembly and the monopolar plate of a proton exchange membrane fuel cell.

2. EXPERIMENTAL METHODS

Recently, digital pressure sensing devices have been made available to researchers. Tekscan digital pressure sensors (Tekscan, Inc., South Boston, MA, USA) are one of the newer available technologies for quantification of compressive loads and contact pressures. These thin-film sensors are manufactured in many different sizes, shapes and range of spatial resolution. Researchers within the field of orthopaedics have used Tekscan sensors to quantify in vitro stress and contact area distributions in the knee joint [8-10] and to measure facet loads in the lumbar spine [11].

2.1. Measuring principle

Tekscan thin-film tactile pressure sensor array is a thin (0,1 mm about) grid-based device. It consists of a matrix of rows and columns of a patented semi-conductive ink coating that changes its electrical resistance when force is applied to it. These rows and columns intersect to form sensing elements (*sensels*) that are sandwiched between two flexible polyester sheets. The pressure on each element is assumed to be constant and equal to the pressure measured at the centre where the piezoresistive strips cross. By electronically scanning and measuring the change in resistance at each individual sensing element, the timing, force and location of contacts on the sensor surface can be determined. Raw (uncalibrated) output can be exported as a 8-bit b/w image.

A Tekscan array model #5076 was used to perform the experimental tests. This array has a square matrix of 83,8 × 83,8 mm consisting of 1936 sensing elements with a spatial density of 27,6 sensel/cm^2 (corresponding to a spatial resolution of about 1,90 × 1,90 mm). The pressure saturation rating (P_{sat}) is 20,7 MPa. When coupled to the I-scan signal conditioning unit, a maximum sampling rate of about 100 Hz can be attained.

Tekscan I-scan software ver. 5.90 was used to gather pressure data and to calculate contact area and force.

2.2. Sensor array calibration

Sensor arrays coming from purchaser are not equilibrated and calibrated, so that equilibration and calibration of the matrix sensels must be performed in order to obtained quantitative data.

These operations were carried out by designing a pneumatic calibration device which allows to apply uniform static pressure levels over the whole sensor area.

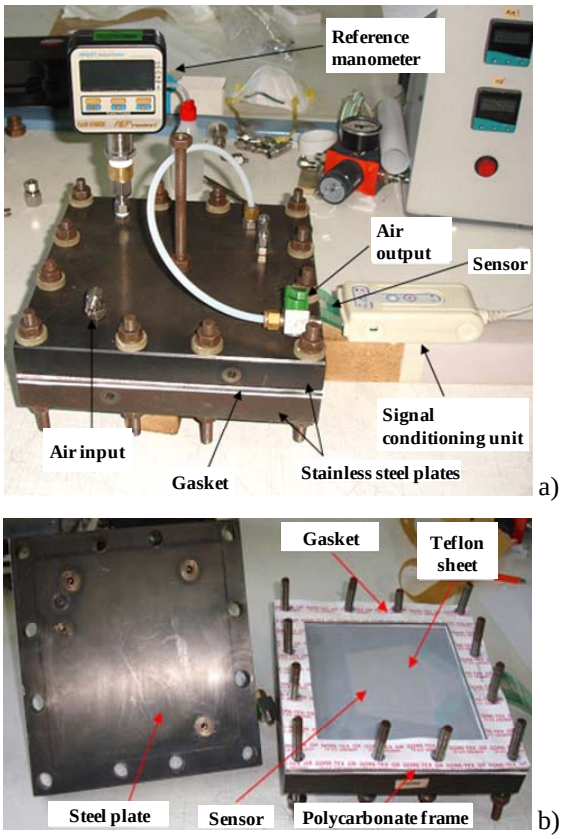

Fig. 1. Static calibration of the thin-film sensor array: a) view of the calibration device with reference pressure meter; b) inside view of the air chamber with the sensor array inserted in it.

The calibration device, see Figs. 1a and 1b, consists of two flat and thick metal plates (planarity tolerance ±5 μm). The film sensor is first placed onto the bottom plate and covered with a thin sheet of Teflon (0,010 mm). Sealing is achieved by means of a Gore-Tex gasket placed over the Teflon membrane. An air chamber was finally obtained by interposing a rigid polycarbonate frame between the two stainless steel plates, which were clamped together by 12×M10 steel bolts. The pressure into the air chamber is controlled by a pressure regulator. A SIT-certified 0,05% accuracy class digital pressure transducer (AEP

Transducers, Modena, Italy), having a resolution of 0,2 kPa, was used as reference pressure meter for the static calibration. Two holes placed in the bottom plate allow the residual air to be driven out from the sensor compartment.

Prior to normalization and calibration, the sensor array was conditioned four times at a pressure of 2000 kPa.

Preliminary tests carried out with Tekscan sensors have shown a significant pillow effect. It was thought that the main source of dumping might be due to air entrapped between the two thin polyester sheets that enclose the electrically conductive patterns of the sensor. Thus, to overcome this problem, small cuttings were made in between traces (inactive area) of the sensor array, allowing trapped air to vent or escape.

Before calibration, the matrix sensor was normalized to compensate for differences in sensitivity between sensels. The sensor was placed into the calibration device and subjected to a uniform pressure level. Then a digital compensation was performed by acting on the gain of each individual sensel, so that its digital level (DL) matched the average digital level of all loaded sensels. After equilibration, the array showed, under a uniform pressure, a residual deviation of ± 2 DL over the whole loaded area (Fig. 2). The equilibration process was repeated at multiple uniform pressure levels to assure a consistent sensor response over the whole range of interest.

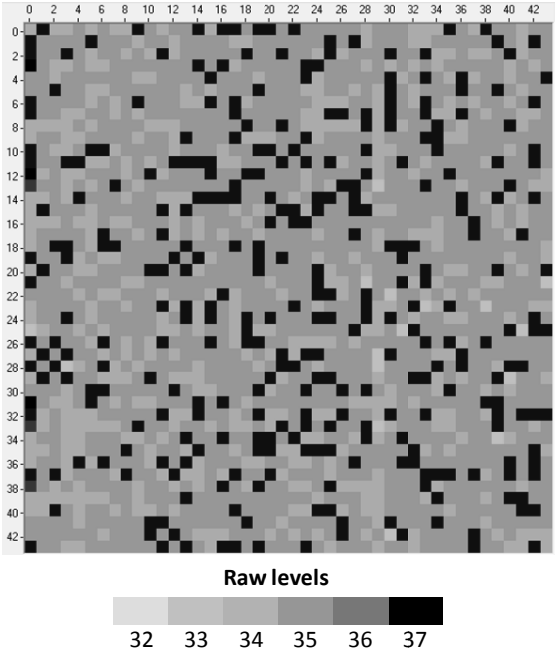

Fig. 2. Sensor equilibration: raw output (digital levels) of the sensor array under a uniform pressure level of 1000 kPa after digital compensation (total number of sensels 44 × 44).

Static calibration of the thin-film sensor array was carried out with both increasing and decreasing pressure steps in the range 0 – 2000 kPa. Throughout calibration, pressures were ramped up over 10 s and held for about 5 s. The calibration test was repeated six times in order to assess repeatability. At each uniform pressure stage the digital output of the array was averaged over all the matrix sensels to get the average raw output (Table 1). Repeatability under increasing pressures resulted better than 3% of the average raw output. As far as reversible pressure loads are taken into account, the sensor array displayed a negligible hystereris, with higher relative errors (Δ) at low pressures.

Table 1. Sensor calibration: average measured raw output under increasing (+) and decreasing (–) pressure loads and relative difference (Δ). Values are in 8-bit digital levels (DL).

Ref. press. (kPa)	Raw (+) (DL)	Std. Dev. (DL)	Std. Dev. (%)	Raw (–) (DL)	Δ (DL)
200	9	0,2	2,1%	10	-0,7
400	17	0,5	2,9%	18	-0,6
600	24	0,6	2,7%	25	-0,6
800	29	0,7	2,4%	30	-0,8
1000	35	0,8	2,2%	36	-0,6
1200	40	0,9	2,3%	41	-0,7
1400	45	0,8	1,8%	46	-0,8
1600	49	1,0	2,1%	50	-0,8
1800	53	1,1	2,1%	54	-0,8
2000	57	1,1	1,9%	57	0,0

Average raw outputs were interpolated using a least squares curve-fitting technique. The sensor array exhibited a markedly non linear trend (Fig. 3), that can be well approximated by a cubic polynomial algorithm (R^2 = 0,998).

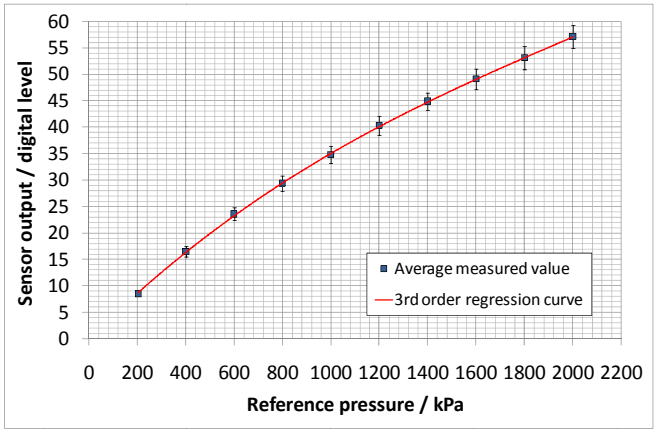

Fig. 3. Sensor calibration: average raw output ± standard deviation (95% confidence level) measured at 10 different reference pressure loads with superimposed least squares curve-fitting.

Following equilibration and calibration, the sensor array was subjected to 3 loading cycles consisting of 10 loads between 200 kPa and 2000 kPa applied in a random order. The sensor remained unloaded for 180 s between load application. Pressure data were saved as raw values and calibrated externally by using the 3rd order regression curve. The root mean square (RMS) error between the calibrated sensor output and the reference pressure load was found to be 93 ± 44 kPa (4,6%).

2.3. Embedding of the sensor array into the fuel cell

The PEMFC (Fig. 4a) used for testing was designed and assembled at the CNR-ITAE Institute. It has a multiple coil flow field with two Cu endplates clamped together by means

of 8×M6 steel bolts. The active area (i.e., area of the membane electrode assembly) is about 50 cm^2, while the total endplate area, which includes the sealing gasket, is about 82 cm^2. Hence, since the active area of the sensor array is smaller than the endplate of the fuel cell, the sensor had to be placed covering only one side of the gasket frame (see Fig. 4b). Moreover, to put up the sensor film into the fuel cell, a hole had to be made on the film itself allowing one of the clamping bolts to be inserted through it.

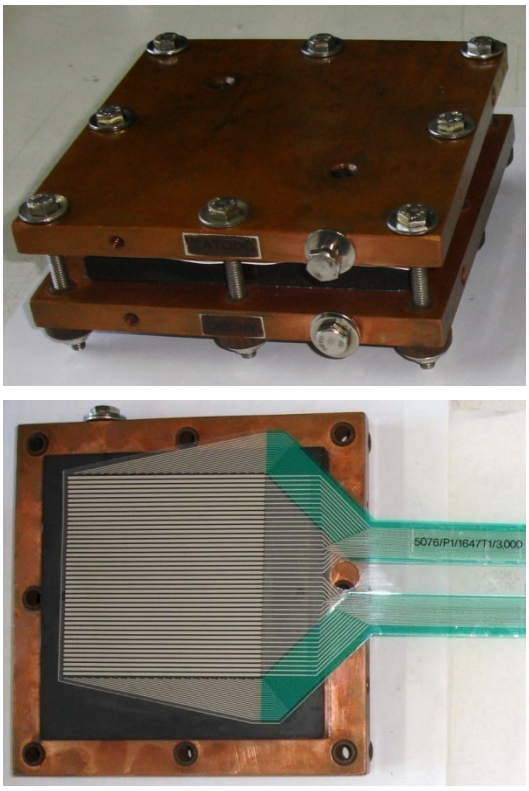

Fig. 4. Proton exchange membrane fuel cell: a) assembled fuel cell; b) positioning of the pressure film onto the MEA.

Experimental tests were carried out by varying the external clamping pressure step by step. This was obtained by using a calibrated torque wrench with torque values of 2, 4, 6, 8, 10 and 11 Nm.
At each step, after waiting for about 30 s, the torque value on each bolt was checked to account for possible gasket or porous membrane electrode relaxations. The eight bolts were clenched using always the same sequence (mid-left, mid-right, mid-lower, mid-upper, upper-left, lower-right, lower-left, upper-right). Measurements were taken waiting 180 s after each step increase or decrease.

3. RESULTS AND DISCUSSION

The obtained results are shown in Fig. 5, where average contact pressures on the membrane electrode assembly, on the sealing gasket and on the end plate are reported as a function of the applied clamping torque. Average values were calculated by considering the whole area of the membrane electrode (MEA), four times the area covered by one side of the seal frame (gasket) and the area of all loaded sensels (end plate), respectively.

It can be observed that the average contact pressure acting on the MEA does not increase significantly as the clamping pressure is raised. Otherwise, the average contact pressure on the gasket displays an initial sharp increase up to 6 Nm, followed by a reduced pressure slope.

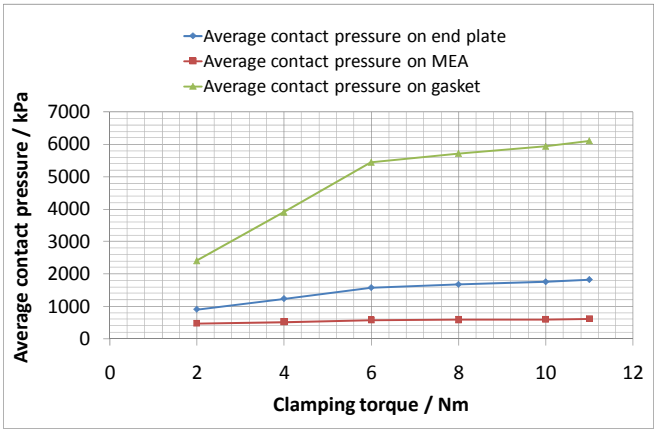

Fig. 5. Average contact pressures measured on fuel cell's MEA, gasket and monopolar endplate at different clamping torques.

Further insight into the actual pressure distribution within the PEMFC can be achieved by observing the colour-coded pressure contours reported in Fig. 6. Although the average pressure on the MEA remains almost constant, its distribution reveals that, as the clamping torque on the endplates is increased, the innermost area of the membrane electrode becomes gradually more unloaded, while, at the same time, average stresses on the gasket rise up, with significant stress concentration around the edge corners. This behaviour proved that the endplates bent under loading, producing an uneven pressure distribution over the fuel cell electrode.

Table 2. Average contact pressures measured at 11 Nm on MEA, gasket and monopolar endplate by changing the relative orientation of the sensor array with respect to the fuel cell (90° steps).

Sensor array orientation	Avg. pressure on MEA (kPa)	Avg. pressure on gasket (kPa)	Avg. pressure on end plate (kPa)
0°	620	6110	1830
90°	588	6286	1765
180°	644	6568	1898
270°	604	6181	1788

Experimental tests were also repeated by rotating the pressure film, changing its relative position with respect to the fuel cell. These tests allowed to check the pressure distribution over all the frame area of the sealing gasket, although values were measured in replicated tests rather than in one single shot. Average pressures are reported in Table 2 while colour-coded pressure distributions are shown in Fig. 7. Both average pressure values and pressure distributions show a limited variability, which is within the uncertainty of the current measurement set-up.

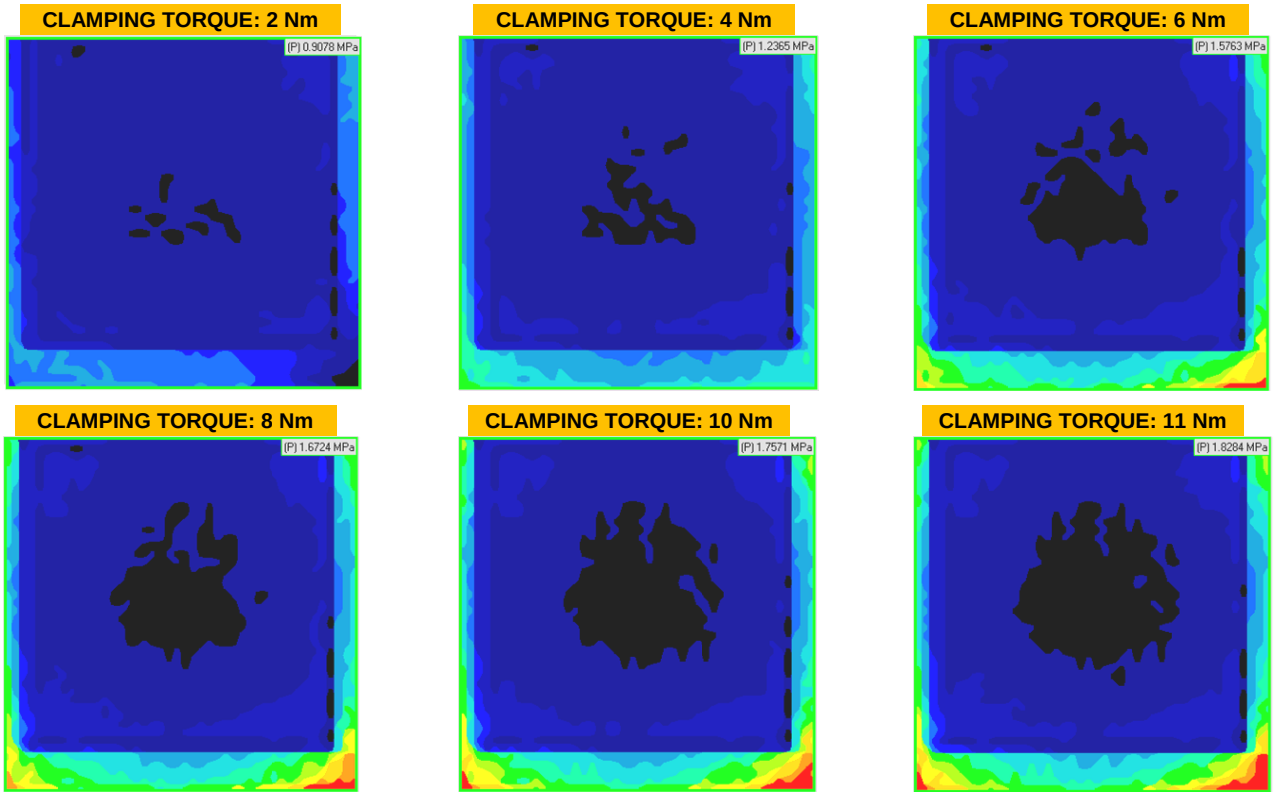

Fig. 6. Colour-coded contours showing measured pressure distribution inside the PEMFC at different clamping torques.

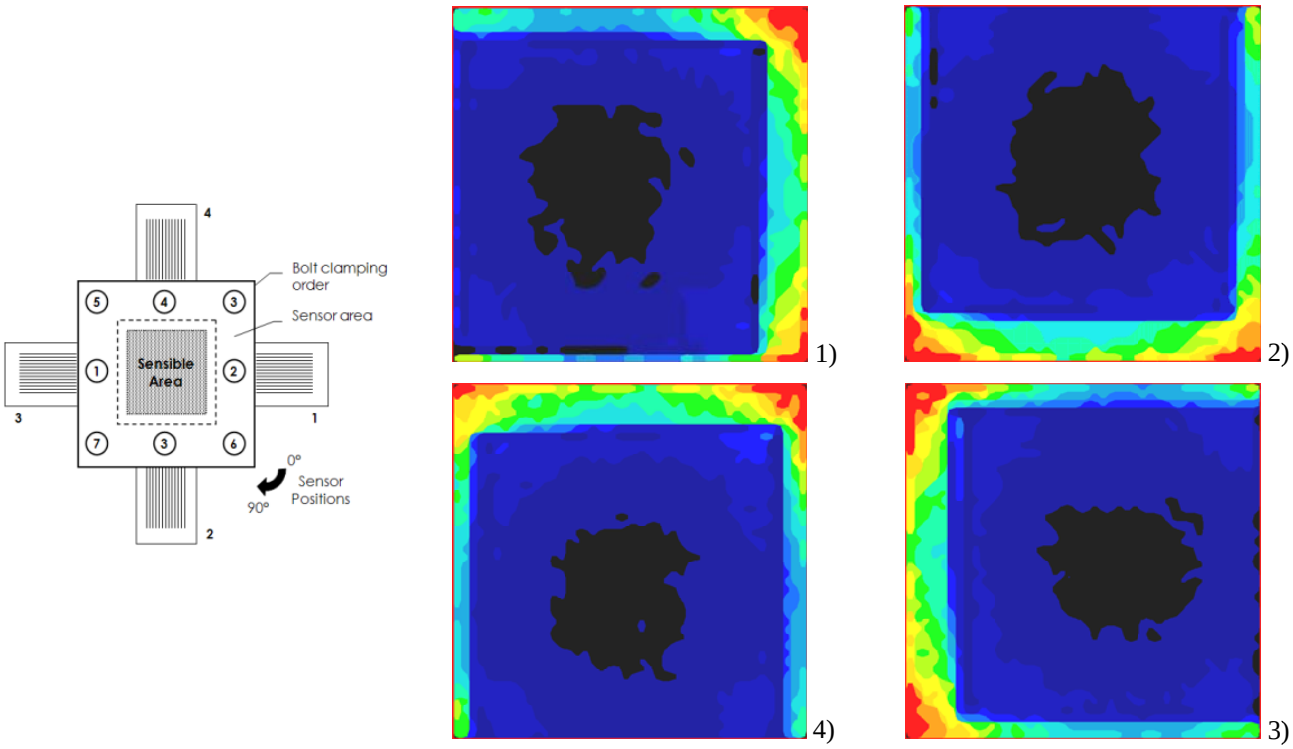

Fig. 7. Colour-coded contours showing pressure distribution at 11 Nm clamping torque obtained by rotating the sensor array with respect to the fuel cell (90° steps).

Whatever the relative position of the film sensor with respect to the fuel cell is, the highest stress value was always found close to the edge corners of the endplate. Moreover, the pressure distribution along the sealing gasket looks quite symmetric.

4. CONCLUSIONS

An experimental approach that allows to measure and monitor the contact pressure distribution within a fuel cell as the clamping pressure is varied has been presented.

The proposed methodology relies on the use of a grid-based piezoresistive thin-film array, which was placed between the membrane electrode and the monopolar endplate of a proton exchange membrane fuel cell.

Preliminary results reported in this study highlight the effectiveness of the proposed measurement solution, which allowed to gain quantitative data about the relationship between the actual pressure distribution within the fuel cell and the applied external clamping torque.

Since an uneven distribution of the contact pressure can result in hot spots which might have a detrimental effect on the electro-chemical performance and life of the PEMFC, this correlation can be of considerable interest for fuel cell stack design. The proposed measurement system may assist the development of next-generation fuel cells or could be used as a powerful validation tool for detailed finite element models.

Future work directions will try to find an evidence on the actual correlation existing between the pressure distribution on the MEA and the electro-chemical performance of the fuel cell.

ACKNOWLEDGMENTS

The Authors would like to thank Fabio Irato for his assistance in performing the experimental tests.

REFERENCES

[1] W.K. Lee, C.H. Ho, J.W.V. Zee, M. Murthy, “The effects of compression and gas diffusion layers on the performance of a PEM fuel cell”, *Journal of Power Sources*, vol. 84, pp. 45–51, 1999.

[2] J. Ihonen, M. Mikkola, G. Lindbergh, “Flooding of gas diffusion backing in PEFCs: physical and electrochemical characterization“, *Journal of Electrochemical Society*, vol. 151, pp. 1152–1161, 2004.

[3] H.S. Chu, C. Yeh, F. Chen, “Effects of porosity change of gas diffuser on performance of proton exchange membrane fuel cell”, *Journal of Power Sources*, vol.123, pp. 1–9, 2003.

[4] D. Chu, R. Jiang, “Performance of polymer electrolyte membrane fuel cell PEMFC stacks”, *Journal of Power Sources*, vol. 83, pp. 128–133, 1999.

[5] W.R. Chang, J.J. Hwang, F.B. Weng, S.H. Chan, “Effect of clamping pressure on the performance of a PEM fuel cell”, *Journal of Power Sources*, vol. 166, pp. 149-154, 2007.

[6] X. Wang, Y. Song, B. Zhang, “Experimental study of clamping pressure distribution in PEM fuel cells”, *Journal of Power Sources*, vol. 179, pp. 305-309, 2008.

[7] S. J. Lee, C.D. Hsu, C.H. Huang, “Analyses of the fuel cell stack assembly pressure”, *Journal of Power Sources*, vol. 145, pp. 353–361, 2005.

[8] D.R. Wilson, M.V. Apreleva, M.J. Eichler, F.R. Harrold, “Accuracy and repeatability of a pressure measurement system in the patellofemoral joint”, *Journal of Biomechanics*, vol. 36, pp. 1909–1915, 2003.

[9] K.N. Bachus, A.L. DeMarco, K.T. Judd, D.S. Horwitz, D.S. Brodke, “Measuring contact area, force, and pressure for bioengineering applications: Using Fuji Film and TekScan systems”, *Medical Engineering & Phisics*, vol. 28, pp. 483-488, 2006.

[10] E.I. Drewniak, J.J. Crisco, D.B. Spenciner, B.C. Fleming, “Accuracy of circular contact area measurements with thin-film pressure sensors”, *Journal of Biomechanics*, vol. 40, pp. 2569–2572, 2007.

[11] D.C. Wilson, C.A. Niosi, Q.A. Zhu, T.R. Oxland, D.R. Wilson, “Accuracy and repeatability of a new method for measuring facet loads in the lumbar spine”, Journal of Biomechanics, vol. 39, pp. 348–353, 2006.